

The influence of focal cerebellar lesions on the control and adaptation of gait

W. Ilg,¹ M. A. Giese,¹ E. R. Gizewski,² B. Schoch³ and D. Timmann⁴

¹Section Computational Sensomotrics, Department of Cognitive Neurology, Hertie Institute for Clinical Brain Research, University of Tübingen, ²Department of Neuroradiology, ³Department of Neurosurgery and ⁴Department of Neurology, University of Duisburg-Essen, Germany

Correspondence to: Winfried Ilg, Section Computational Sensomotrics, Department of Cognitive Neurology, Hertie Institute for Clinical Brain Research, Fröndbergstrasse 23, 72076 Tübingen, Germany
E-mail: winfried.ilg@uni-tuebingen.de

Cerebellar ataxic gait is influenced greatly by balance disorders, most likely caused by lesions of the medial zone of the cerebellum. The contributions of the intermediate and lateral zone to the control of limb dynamics for gait and the adaptation of locomotor patterns are less well understood. In this study, we analysed locomotion and goal-directed leg movements in 12 patients with chronic focal lesions after resection of benign cerebellar tumours. The extent of the cortical lesion and possible involvement of the cerebellar nuclei was determined by 3D-MR imaging. The subjects (age range 13–39 years, mean 20.3; seven female; ICARS score: mean 5.7, SD 6.3) performed three tasks: goal-directed leg placement, walking and walking with additional weights on the shanks. Based on the performance on the first two tasks, patients were categorized as impaired or unimpaired for leg placement and for dynamic balance control in gait. The subgroup with impaired leg placement but not the subgroup with impaired balance showed abnormalities in the adaptation of locomotion to additional loads. A detailed analysis revealed specific abnormalities in the temporal aspects of intra-limb coordination for leg placement and adaptive locomotion. These findings indicate that common neural substrates could be responsible for intra-limb coordination in both tasks. Lesion-based MRI subtraction analysis revealed that the interposed and the adjacent dentate nuclei were more frequently affected in patients with impaired compared to unimpaired leg placement, whereas the fastigial nuclei (and to a lesser degree the interposed nuclei) were more frequently affected in patients with impaired compared with unimpaired dynamic balance control. The intermediate zone appears thus to be of particular importance for multi-joint limb control in both goal-directed leg movements and in locomotion. For locomotion, our results indicate an influence of the intermediate zone on dynamic balance control as well as on the adaptation to changes in limb dynamics.

Keywords: cerebellum; locomotion; adaptation; intra-limb coordination; brain imaging

Abbreviations: CP = patients with cerebellar lesions; HC = healthy controls; IB = impaired balance in gait; ICARS = International Cooperative Ataxia Rating Scale; IL = impaired leg placement; ND = dentate nuclei; NI = interposed nuclei; NIB = unimpaired balance in gait; NIL = unimpaired leg placement; ROI = region of interest

Received December 21, 2007. Revised September 2, 2008. Accepted September 8, 2008. Advance Access publication October 3, 2008

Introduction

The contribution of the cerebellum to the control of limb dynamics, including the adaptation to movement perturbations, has been examined mainly for goal-directed arm movements (Hallett and Massaquoi, 1993; Bastian *et al.*, 1996; Topka *et al.*, 1998; Maschke *et al.*, 2004; Diedrichsen *et al.*, 2005; Smith and Shadmehr, 2005). For cerebellar ataxic gait, the influence of impaired balance control is well established (Palliyath *et al.*, 1998; Stolze *et al.*, 2002; Morton and Bastian, 2003). In contrast, cerebellar contributions

to limb coordination for human locomotion are less clear. Recently, Ilg *et al.* (2007) have provided evidence that impairments of intra-limb coordination in ataxic gait are directly influenced by deficits in the control of limb dynamics, rather than being a by-product of balance impairments. The involvement of the cerebellum in the adaptation of locomotion has been shown in different setups such as obstacle avoidance (Morton *et al.*, 2004), perturbed treadmill walking (Rand *et al.*, 1998), or walking on a splitbelt treadmill (Morton and Bastian, 2006). Since the existing human studies

have been conducted predominantly in patients with degenerative cerebellar diseases, no claims can be made about the responsible anatomical structures. Animal studies suggest that balance control is located in the medial zone including vermis and fastigial nuclei (NF) (for reviews see Thach *et al.*, 1992; Armstrong *et al.*, 1997; Thach and Bastian, 2004). Mechanisms for the control of limb dynamics in goal-directed movements are hypothesized to be located mainly in the intermediate zone consisting of paravermal regions and interposed nuclei (NI) as well as in the lateral zone including cerebellar hemisphere and dentate nucleus (ND).

In principle, clinical observations confirm this functional categorization (Dichgans and Diener, 1984). However, in humans few attempts have been made to differentiate between the function of the intermediate and lateral zone. Two recent studies on patients with focal cerebellar lesions due to surgery and stroke showed that the NI as well as adjacent parts of the ND are related to the degree of upper- and lower-limb ataxia (Konczak *et al.*, 2005; Schoch *et al.*, 2006).

In this study we analysed locomotion and goal-directed lower limb movements in 12 patients with chronic focal lesions after resection of benign cerebellar tumours. This study has two main objectives: first, the analysis of influences of impaired balance control and intra-limb coordination for three movements: voluntary leg placement, locomotion and the adaptation of locomotor patterns, where the limb dynamics was changed by adding weights to the shanks. We focused in particular on the analysis of the spatio-temporal characteristics of intra-limb coordination and examined whether patients with impaired leg placement also show deficits in adaptive locomotion. Such a pathophysiological association would support the hypothesis that common neural substrates are responsible for the intra-limb coordination in both tasks.

The second goal of the study was to investigate the mapping between observed impairments and the neuro-anatomy of lesion sites. We hypothesized that lesions of the medial zone would induce disordered balance control in gait, whereas the intermediate and/or lateral zone would be of more importance for leg placement and gait adaptation.

Methods

Subjects

We analysed 12 patients (CP 1–12) with chronic focal lesions after cerebellar tumour resection (age range 13–39 years, mean 20.3; seven females; ICARS score: mean 5.7, SD 6.3) and an age-matched control group (five females, age range 13–39 years, mean 20.3). All patients suffered from benign cerebellar tumours [pilocytic astrocytoma WHO grade I ($n=9$), haemangioblastoma ($n=2$) or cavernoma ($n=1$)] and none of the patients received adjuvant radio- or chemotherapy (Table 1).

All patients showed mild symptoms of ataxia and were able to walk without aid. To determine leg dominance, we asked subjects which leg they prefer for kicking a ball and which leg they put forward to balance themselves when pushed from behind. Each subject was examined by an experienced neurologist (D.T.). Severity of ataxia was rated using the International Cooperative Ataxia Rating Scale (ICARS) (Trouillas *et al.*, 1997). None of the patients with cerebellar lesions revealed extracerebellar signs except a suspicious Babinski's sign on the right in CP8 and right abducens nerve palsy in CP6. Standard neurological examination included testing of the vibration sense (tested at the medial malleolus) and joint-position sense (tested at the hallux metatarsophalangeal joint), both revealing no abnormalities.

All patients and control subjects gave informed consent prior to participation. In the case of adolescents, the adolescent and his or her legal guardians gave their informed consent. The study had been approved by the local institutional ethical review board.

Table 1 Cerebellar subject information

	Age (years)	Time post-op (months)	Diagnosis	ICARS				
				Total (max. 100)	Gait (max. 12)	Posture (max. 18)	Lower limb (max. 16)	Upper limb (max. 36)
CP1	21	110	Cavernoma	0	0	0	0	0
CP2	18	36	Astro I	0	0	0	0	0
CP3	39	10	Haemangioblastoma	4	0	1	0	3 (r)
CP4	19	110	Astro I	14	1	2	1 (r)	6 (r)
CP5	14	133	Astro I	14	1	3	1 (r)	6 (r)
CP6	19	70	Astro I	17	1	3	1 (r)	9 (r)
CP7	16	113	Astro I	3	1	1	0	1 (r)
CP8	27	18	Haemangioblastoma	0	0	0	0	0
CP9	13	103	Astro I	5	1	2	0	2 (r)
CP10	21	67	Astro II	1	1	0	0	0
CP11	20	18	Astro I	3	0	1	0	2 (l)
CP12	16	84	Astro I	6	1	2	0	3 (l)

Clinical scores were rated using the ICARS score (Trouillas *et al.*, 1997). The table lists the total ICARS scores and the relevant subscores for posture, gait and limb kinetics. Higher scores indicate more severe ataxia. Maximum scores are given in brackets. (r) and (l) denote the affected side in ataxia limb scores. Astro I = pilocytic astrocytoma WHO I, Astro II = astrocytoma WHO II.

Experimental paradigm

All subjects performed the three following tasks in the order: goal-oriented leg placement, normal walking and walking with additional weights on the shanks. Based on their performance on the first two tasks, patients were categorized as impaired or unimpaired in leg placement (parameter: mean end-point error) as well as in balance in gait (parameters: step width, lateral sway). Categorization was determined by generating 99% confidence intervals from the control group. Patients whose values fell outside the confidence interval for the corresponding parameter were categorized as impaired on this task.

The third task was designed to study the behaviour of the different patient subgroups on the adaptation of locomotor patterns to changes of limb dynamics, achieved by placing additional weights on the shanks.

For all tasks we analysed the performance of both legs separately, in order to determine the influence of focal lesions on the ipsi-lateral and the contra-lateral leg.

Voluntary leg placement

Subjects had to step on a visual target (diameter 3 cm) on the floor with the toe of the stepping leg. At the beginning of each trial, subjects stood with both feet approximately shoulder-width apart and with the toe of their stepping leg about one foot length behind the stationary leg. The target was located one step length in front of the stepping leg. Stepping distances were adjusted to leg length, so that subjects were able to reach the target comfortably with one step. Subjects performed the task while holding on to short rails placed on the right and left side of the body, reducing the potential effects of balance deficits (Sullivan *et al.*, 2006). This experimental setup is comparable to that described by Morton and Bastian (2003). The experiment was performed with both legs executing 10 trials per leg. Since control subjects show lower leg placement error for their preferred foot, confidence intervals were computed for the preferred and the non-preferred foot separately. The subjects were barefooted during all movement tasks.

Normal gait

Patients were instructed to walk normally at a self-determined speed on a 12 m pathway. From each patient 15–20 gait cycles were recorded, assessed within three to five experimental trials. For the categorization of balance impairments in gait we analysed step width and lateral sway. There was a significant correlation between step width and the ICARS posture subscore ($r = 0.61$, $P = 0.03$).

Gait with additional weights on the shanks

To examine adaptation to changes in limb mechanics, additional weights (1 kg) were attached to both shanks ('adaptation trials'). Subjects performed three trials, each with ~10 gait cycles per trial. The weights were then removed, and subjects performed three additional trials in order to test for after-effects ('post-adaptation trials'). Between trials, patients returned to the starting point walking across the pathway in the other direction without recording of their movements. Subjects were instructed not to move their feet before starting the first trial of the adaptation and post-adaptation trials. In Noble and Prentice (2005), it was shown that on a treadmill the full adaptation process for healthy subjects takes between 45 and 50 strides. Thus, we assumed that the adaptation

to the weight should have been completed in the third walking trial for healthy subjects.

Recording of movement trajectories and preprocessing

The three-dimensional movement trajectories of the patients were recorded at a sampling rate of 120 Hz using a VICON 612 motion capture system with 10 cameras and 41 reflecting markers. The marker trajectories were preprocessed using the commercial software provided by VICON. This software fits a clinically evaluated kinematic model to the marker trajectories and extracts velocities, joint angles and the course of the centre of mass (CoM).

Gait cycles were automatically determined from the trajectories by detection of heel-strike events, based on the vertical components of the heel marker positions. Results of the automatic detection were verified manually using a stick figure animation in order to correct for different types of foot placement.

We computed several parameters of clinical gait analysis (Kirtley, 2006). Step width was measured by determining the lateral distance between the right and left heel markers at the time of heel strike. Step length was normalized for body height. Lateral body sway was defined as the lateral component of the path of the centre of mass (CoM), normalized to the anterior–posterior component for each trial.

The reconstructed joint angle trajectories were smoothed with a Savitzky-Golay polynomial filter (of order four and with a window size of 41 sampling points) and resampled equidistantly with 100 data points per gait cycle by linear time interpolation. In this study, we focused on the analysis of the joint coordination pattern for hip and knee motion in the sagittal plane (flexion/extension). This joint combination has been shown to be most indicative for changes in intra-limb coordination in previous studies (Morton and Bastian, 2003; Ilg *et al.*, 2007) [in Morton and Bastian (2003) the decomposition index in gait for the pair of hip and knee joints was significantly increased for the patient group exhibiting impairments in voluntary leg placement]. For the computational analysis the angle trajectories of all gait cycles were normalized to a common angle interval (range 0–1) for each subject separately in order to compensate for amplitude variations between different joints.

Quantification of the spatio-temporal characteristics for intra-limb coordination patterns

In previous work (Ilg *et al.*, 2007) we have introduced spatio-temporal correspondence (Giese and Poggio, 2000) as a basis for quantitative analysis of multi-joint coordination patterns. In particular, such correspondence-based measures permit the detection of specific temporal abnormalities in intra-limb coordination in patients with cerebellar dysfunctions (Ilg *et al.*, 2007). These abnormalities resemble deficits in the temporal structure of intra-limb coordination caused by cerebellar lesions in animal studies (Milak *et al.*, 1997; Cooper *et al.*, 2000). A quantification of these specific temporal abnormalities has been accomplished by the separation of the temporal and the spatial trajectory characteristics, while common variability measures (for review see e.g. Stergiou, 2004) failed to detect these abnormalities reliably.

Figure 1A illustrates the principle underlying this method for the one-dimensional case. Spatio-temporal correspondence is defined by a set of spatial and temporal displacements that map

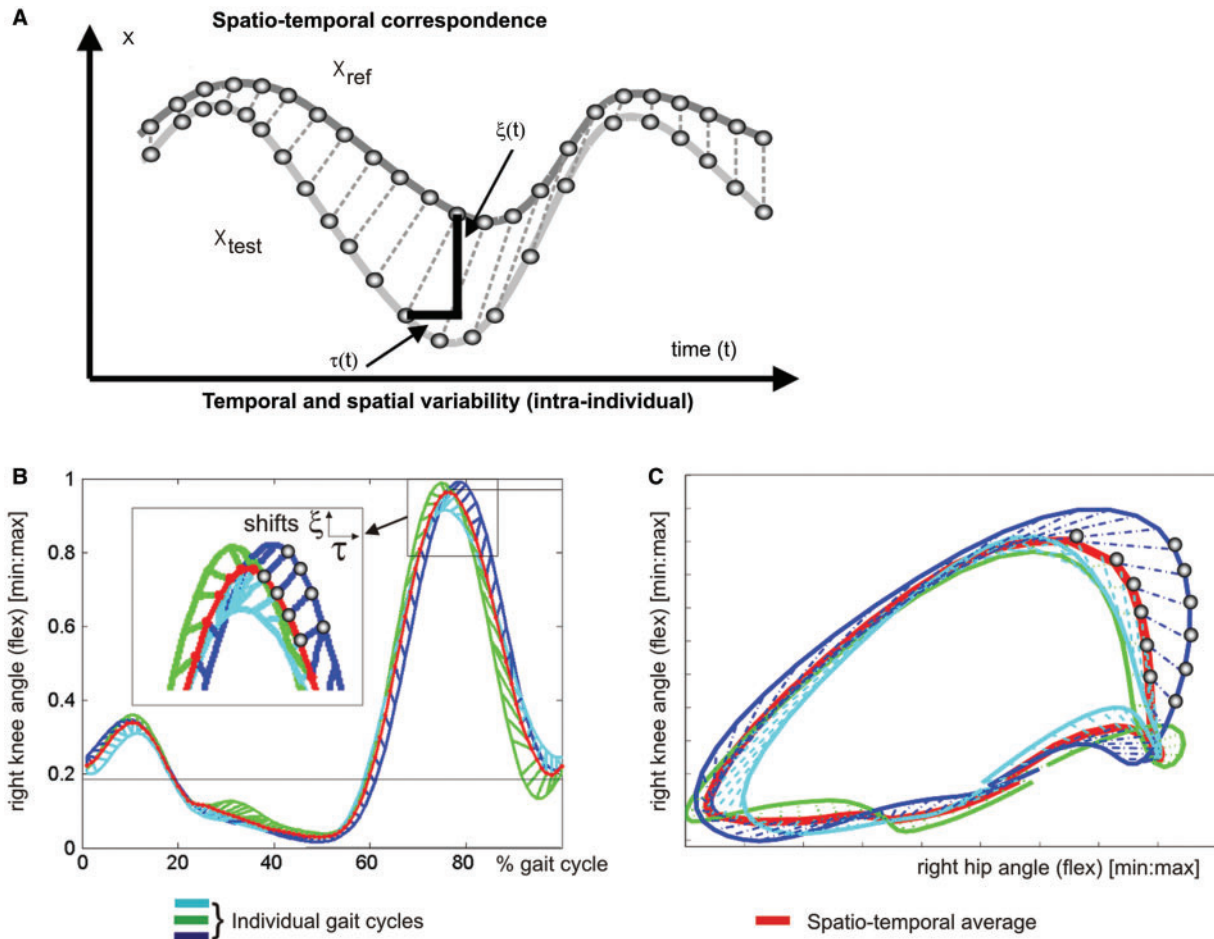


Fig. 1 (A) Illustration of spatial–temporal correspondence between a reference trajectory and a test trajectory. Circles indicate corresponding points of the two trajectories. The spatio-temporal displacements between corresponding points (indicated by dashed lines) have spatial and temporal displacement components, defining the correspondence fields $\xi(t)$ and $\tau(t)$. (B) Illustration of spatial and temporal variability for real data and computation of the average movement for the gait trajectories of a cerebellar patient. Joint angle trajectories are shown for the right knee flexion angle for three gait cycles. Thin lines between the trajectories connect points that are in spatio-temporal correspondence. Note, that the explicit representation of temporal and spatial characteristics allows a more adequate differentiation between spatial and temporal errors (see box). (C). Analysis of spatial and temporal inter-subject variability of two-dimensional joint angle trajectories. Trajectories are illustrated using an angle-angle plot. A spatio-temporal average trajectory is computed over three trajectories from individual gait cycles of the same patient.

a test trajectory $x_{\text{test}}(t)$ onto a reference trajectory $x_{\text{ref}}(t)$. The circles on the trajectories that are connected by dashed lines indicate points that are in spatio-temporal correspondence, for example the maxima of the two trajectories. Each point $x_{\text{ref}}(t_n)$ on the reference trajectory corresponds to a point $x_{\text{test}}(t_n)$ on the test trajectory. The points are displaced against each other in space by the spatial vector $\xi(t_n)$ and in time by the (scalar) time shift $\tau(t_n)$. The two displacement functions $\xi(t)$ and $\tau(t)$ characterize the spatio-temporal deviation of the test trajectory from the reference trajectory and decompose it into a spatial and a temporal component (Fig. 1B).

The correspondence algorithm determines these displacement functions by minimizing an error function that is given by a weighted sum of the time integrals of the squared spatial and temporal displacements:

$$E(\xi, \tau) = \int \left(|\xi(t)|^2 + \lambda \tau(t)^2 \right) dt \quad (1)$$

The positive constant λ determines the relative contributions of spatial and temporal differences to this error. For the current analysis the parameter was set to $\lambda = 0.004$. In the Supplementary information we provide an analysis, showing that the presented results are valid for a wide range of the parameter λ .

The algorithm for the minimization of the error function in Equation (1) (Giese and Poggio, 2000) is also briefly described in the Supplementary information. Note, that since the trajectories $x(t)$ and the spatial vector $\xi(t)$ can in principle have an arbitrary number of spatial dimensions, these measures can be applied to multi-dimensional joint coordination patterns. Figure 1C shows the application for a two-dimensional coordination pattern. Based on this spatio-temporal representation, measures of spatial and temporal variability of the movements are determined by separately averaging the spatial and temporal deviations from reference trajectories. Reference trajectories $x_{\text{ref}}(t)$ were computed separately for each participant, and were defined by the space–time average of all gait cycles $x_k(t)$ from the same subject. Separate measures

of spatial and temporal variability were constructed by averaging the absolute values of the spatial shifts $\xi_k(t)$ and of the temporal shifts $\tau_k(t)$ over all gait cycles (K signifying the number of recorded gait cycles and T the gait cycle time):

$$vb_{\xi} = \frac{1}{K} \sum_{k=1}^K \int_0^T |\xi_k(t)| dt$$

$$vb_{\tau} = \frac{1}{K} \sum_{k=1}^K \int_0^T |\tau_k(t)| dt$$
(2)

We compare our spatio-temporal measures with a common measure of pure spatial variability vb_s (see Supplementary information).

In order to analyse the changes in intra-limb coordination for walking with weights compared to walking without weights, we computed temporal and spatial shifts between the adaptation trials and an average trajectory from pre-adaptive walking without weights as reference, indicated by $\xi_k^{\text{ad}}(t)$ and $\tau_k^{\text{ad}}(t)$. The corresponding variability measures are:

$$vb_{\xi}^{\text{adapt}} = \frac{1}{K} \sum_{k=1}^K \int_0^T |\xi_k^{\text{ad}}(t)| dt$$

$$vb_{\tau}^{\text{adapt}} = \frac{1}{K} \sum_{k=1}^K \int_0^T |\tau_k^{\text{ad}}(t)| dt$$
(3)

Correspondingly, the measures vb_{ξ}^{post} and vb_{τ}^{post} quantify the differences in intra-limb coordination between the pre- and the post-adaptation trials without weights.

In addition, this representation can be applied to the analysis of intra-limb coordination during specific phases of the gait cycle (e.g. swing phase), by restricting the analysis of the spatial and temporal shifts to the given phase.

Imaging procedures and measures

The extent of surgical lesions was defined by individual three-dimensional (3D) MRI data sets acquired on the same day as behavioural testing was performed. A 3D sagittal volume of the entire brain was acquired using a T_1 -weighted MPRAGE sequence (FOV = 256 mm, number of partitions = 160, voxel size = $1.00 \times 1.00 \times 1.00 \text{ mm}^3$, TR/TE = 2400/4.38 ms, flip angle = 8°) on a Siemens Sonata 1.5 T MR scanner. In addition, axial and sagittal two-dimensional T_2 -weighted images of the entire brain were acquired. MPRAGE and T_2 -weighted images were visually examined by an experienced neuroradiologist (E.G.). None of the patients revealed extracerebellar pathology.

Surgical lesions were manually traced on axial, sagittal and coronal slices of the non-normalized 3D-MRI data set and saved as region of interest (ROI) using MRICro software (<http://www.sph.sc.edu/comd/rorden/micro.html>). Spatial normalization into standard proportional stereotaxic Montreal Neurological Institute (MNI) space was performed according to the masking technique described by Brett *et al.* (2001) using SPM2 (<http://www.fil.ion.ucl.ac.uk/spm/>; Wellcome Department of Cognitive Neurology, London, UK)

The MPRAGE volume was registered and resampled to $2.00 \times 2.00 \times 2.00 \text{ mm}^3$ voxel size. Because the process of spatial normalization is likely to introduce some errors in individual anatomy, particularly within the posterior fossa, the extent of individual lesions was also analysed based on non-normalized data

for each individual subject, using characteristic anatomical landmarks. Normalized regions of interest were manually adjusted, if the normalization introduced spatial errors that would lead to incorrect localization. The researcher (B.S.) conducting the MRI analysis was unaware of the behavioural data.

Based on the MNI spatial coordinates of cerebellar lesions the corresponding cerebellar lobules were defined with the help of 3D-MRI atlases of the cerebellum (Schmahmann *et al.*, 2000) and the cerebellar nuclei (Dimitrova *et al.*, 2002). Lesions of vermis, paravermis and lateral hemispheres were considered separately (Schoch *et al.*, 2004).

In eight patients lesions affected the cerebellar vermis and in the other four patients lesions were restricted to the cerebellar hemispheres. All patients showed affection of the cerebellar hemispheres to various degrees, with the left hemisphere being exclusively or predominantly affected in patients CP8, CP11 and CP12, and the right hemisphere in the others. Cerebellar nuclei were affected to various degrees in all patients except two (CP2 and 8) (see Table 2 for a detailed lesion description).

To identify cerebellar regions related to balance and leg placement control, ROI subtraction analysis was performed in MRICro (<http://www.sph.sc.edu/comd/rorden/micro.html>) (Karnath *et al.*, 2002; Rorden *et al.*, 2007). As outlined above, ROIs refer to the 3D-MRI volume of each patient's lesion located in MNI space. For subtraction of ROIs, right-sided lesions were flipped to the left.

Based on behavioural cut-offs (see below) patients were divided into (i) subgroups with and without impaired balance in gait (IB and NIB), and (ii) subgroups with and without impaired leg placement (IL and NIL).

The logic and power of ROI subtraction analysis is described in detail in Karnath *et al.* (2002). First, the lesions for all patients impaired in a given task (IB or IL) are added together, creating a traditional overlap image showing the regions of mutual involvement. Next, the lesions for the unaffected patients (NIB or NIL) are subtracted from the affected group's overlap image. This method creates an image showing which brain regions are affected commonly in different groups. Positive values indicate regions that are commonly damaged in IB (IL) patients, but that are spared in NIB (NIL) patients. Negative values indicate the reverse situation: regions specifically damaged in the NIB (NIL) patients. Zero values indicate regions that are damaged in equal proportions in IB compared with NIB, and IL compared with NIL. The results of this analysis are illustrated in Figs. 3 and 4. Brighter shades of red, orange and yellow highlight positive values and progressively brighter shades of blue illustrate negative values. Regions with a value of zero are shown in purple. The percentage subtraction plots show 11 'levels' of ROI: each bar represents 20% increments with yellow representing 81–100% affected group. The lightest blue represents 81–100% unaffected group and the middle purple percentage bar designates regions where there is an identical per cent of affected and unaffected groups (0%). Cerebellar regions with the highest relative percentages of the number of ROIs in the impaired group were analysed based on MRI coordinates as outlined above.

Statistical analysis

Group differences between patients and HC were confirmed by Mann–Whitney U-tests (non-parametrically) and independent-samples *t*-tests (parametrically). Non-parametric tests were used for the comparison of patient subgroups with small sample sizes

Table 2 Neuroanatomical location and volume of individual lesions

Subject	Vermal	Paravermal	Lateral hemispheres	White matter	Cerebellar nuclei	Volume (cm ³)
CPI		r: CR I	r: CR I	r: PV I–3 r: H	ND r	2.6
CP2			l: CR I, CR II			2.6
CP3		r: V, VI	r: VI, CR I, CR II, VIIB	r: PV I, 2 r: LH r	ND r	5.8
CP4	VIIAt–X	r: VIIA–IX	r: VIIIA	V 2, 3 r: PV 2, 3 r: H	NI r ND r NF r	12.0
CP5	III, IV, VIIAt–IX	r: III–VI, CR II–VIII B	r: V, VI, VII B, VIII A	V I–3 r: PV I–3 r: H	NF b NI r ND r	20.3
CP6	III, VIIAt–IX			V I–3 r: PV I–3	NF b NI r ND r	9.5
CP7	VIIAt–X			V I–3	NF b NI b	7.4
CP8			l: CR I, CR II	l: PV 2		4.8
CP9	III–X	r: V–IX	r: VII B	V I–3 r: PV I–3	NF b NI b ND r	17.4
CP10	V–VIIB,	r: VI		V I, 2 r: PV 2	NF b NI b	8.0
CPII		l: CR II–VIIIA	l: CR I–VIIIA	l: PV 2, 3	ND I	4.2
CPI2	III–X	l: VI	l: VI, CR I	V I–3 l: PV 2, 3	NF b NI b ND I	14.6

r = right side, l = left side, b = bilateral, V = vermis, PV = paravermal, H = lateral hemisphere.

Lesion volumes were calculated based on normalized individual lesions. I,2,3 refer to the white matter of lobules I to V, VI and VII, and VIII to X respectively.

or if data were not normally distributed (Kolmogorov–Smirnov test). Significances are reported for group differences with significance level $*P < 0.05$. In addition, Bonferroni adjustment (adjusted $**P = 0.017$) was used to correct for the three pairwise comparisons between (i) controls and patients, (ii) patient subgroups with and without impaired balance in gait, (iii) patient subgroups with and without impaired leg placement. Correlations between the different gait measures and the clinical ataxia rating scale ICARS were computed using Spearman rank correlation.

In order to rule out the possibility that the observed changes in intra-limb coordination were induced by differences in gait velocity, we performed correlation analyses between gait velocity and our variability measures (see Supplementary information). In addition, in order to estimate the effect of cerebellar deficits independently of a possible influence of gait velocity we directly examined the influence of velocity on the adaptation of intra-limb coordination. This was done by performing an univariate ANCOVA (analysis of covariance) with an index of adaptation as independent variable.

In the ANCOVA model group classification (impaired/non-impaired leg placement) was entered as fixed factor and velocity as covariate (see Supplementary information). Statistical analysis was performed using the software packages MATLAB and SPSS.

Results

Voluntary leg placement

The 99% confidence interval for the control group defined cut-off criteria for the mean foot-end-point error. If the mean foot-end-point error exceeded 15.9 mm for the preferred, or 19.4 mm for the non-preferred foot, patients were classified as impaired with respect to the leg placement task. Patients were categorized in subgroups IL or NIL (Table 3). All impaired patients except CP11 (left-sided lesion, see Table 2) were affected in the right leg. CP4 and CP12 showed impairments for both legs. Figure 2A exemplarily

Table 3 Overview of elementary gait and movement parameters and the categorization in patient subgroups according to impairments in balance control in gait (IB/NIB) and leg placement (IL/NIL)

	Standard gait parameters				Leg placement			Impairment category	
	Velocity (m/s)	Step length (cm)	Step width (cm)	Lateral sway	Pref. foot	r (cm)	l (cm)	IB/NIB	IL/NIL
CP1	1.16	64.1 ± 2.4	7.5 ± 2.4	34.7	r	2.11	1.75	NIB	IL
CP2	1.24	71.1 ± 2.7	5.1 ± 2.8	37.1	l	1.18	1.3	NIB	NIL
CP3	0.95	52.7 ± 9.7	9.3 ± 3.3	65.7	r	2.21	1.37	IB	IL
CP4	1.1	58.1 ± 3.8	11.8 ± 4.1	126.8	r	2.53	2.18	IB	IL
CP5	0.89	53.1 ± 3.2	13.4 ± 1.8	92.2	l	2.21	1.56	IB	IL
CP6	1.49	72.3 ± 3.4	13.5 ± 4.2	53.2	l	1.34	1.54	IB	NIL
CP7	1.17	57.2 ± 3.2	12.4 ± 3.2	46.7	r	1.56	1.87	IB	NIL
CP8	1.27	63.6 ± 2.5	8.2 ± 2.4	29.18	r	1.36	1.8	NIB	NIL
CP9	1.24	62.8 ± 3.9	4.7 ± 1.8	31.3	l	1.77	1.71	NIB	IL
CP10	0.93	56.7 ± 1.8	4.7 ± 3.3	30.3	r	2.44	1.91	NIB	IL
CP11	1.28	62.4 ± 2.2	5.3 ± 1.9	25.1	r	1.49	2.29	NIB	IL
CP12	1.1	61.9 ± 4.9	8.9 ± 5.0	71.4	r	1.99	2.31	IB	IL

Balance impairment is categorized according to step width and lateral sway, leg placement according to the mean error in leg placement. For the categorization of leg placement, preferred foot (pref. foot) and non-preferred foot were analysed separately. For step length and step width mean values and SD are given.

shows the foot-end-point errors for patient CP4 and a healthy control subject.

Group comparisons of the leg placement error revealed significant differences between HC and CP ($U = 34$, $P = 0.04$), and between the patient subgroups IL and NIL ($U = 10$, $P = 0.004$) for the impaired leg. The foot-end-point error in the sagittal plane was significantly higher for the IL group (compared to NIL, $U = 12$, $P = 0.01$), but not for the IB group (compared with NIB). In addition, for the IL patients there was a significant performance difference in terms of leg placement error between legs ($t_{10} = 2.20$, $P = 0.03$) (Fig. 2B).

The quantitative analysis of the intra-limb coordination pattern (Fig. 2C) also revealed a significant difference between the patient subgroups IL and NIL for the temporal characteristics of the hip–knee coordination vb_{τ} ($U = 14$, $P = 0.0485$). In contrast the spatial variability measures vb_{ξ} and a common pure spatial variability measure vb_{δ} showed no significant differences. In addition, there was no significant difference for the measure vb_{τ} comparing the patient subgroups IB and NIB. These results indicate that the increased temporal variability vb_{τ} not only reflects an increased spatial error, but a specific impairment in temporal aspects of intra-limb coordination.

Voluntary leg placement—brain imaging analysis

Lesion sites in the subgroup of patients with impaired leg placement included the interposed and adjacent dentate nuclei on the affected side to a higher percentage compared to the subgroup with unimpaired leg placement (Fig. 3). Subtraction of the individual ROIs of the eight patients with impaired leg placement and the four patients with unimpaired leg placement showed that affection of dorsomedial parts of the dentate nucleus was 41–60% more common in the impaired group (red colour;

MNI coordinates: $x = -12$ to -8 mm, $y = -64$ to -56 mm, $z = -38$ to -34 mm) (Dum and Strick, 2003). Please note that the colour bars show percentage subtraction in eleven levels of ROI: each bar represents 20% increments with yellow representing 81–100% of the impaired group (and light blue 81–100% of the unimpaired group). Affection of the interposed nucleus was 21–40% more common in the impaired group (middle brown; MNI coordinates: $x = -26$ to -6 mm, $y = -64$ to -54 mm, $z = -42$ to -26 mm). This region included parts of the adjacent dentate nucleus and vermal lobules V and VI ($x = 0$ to 4 mm, $y = -70$ to -52 mm, $z = -28$ to -22 mm).

Balance control in gait

The 99% confidence interval for the control group defined a cut-off criterion for step width of 8.5 cm and of 38.3 cm for lateral sway. We obtained the same categorization results for both balance-related parameters (Table 3). Patients were categorized in subgroups of IB and NIB.

Balance control—brain image analysis

Lesion sites in the NF and lower vermis were more common in the impaired balance subgroup than in the subgroup with unimpaired balance in gait. Subtraction of the ROIs of the six patients with impaired balance control and the six patients with unimpaired balance control (see Fig. 4), showed that affection of the NF and lower vermis was 61–80% more common in the impaired group [light orange; MNI coordinates: NF ($x = -2$ to $+2$ mm, $y = -48$ to -52 mm, $z = -26$ to -30 mm), vermal lobule VIIIIB ($x = 0$ to $+4$ mm, $y = -58$ to -64 mm, $z = -42$ to -46 mm)]. A more extended area was 41–60% more common in the affected group (red colour). This area included the fastigial and interposed nucleus and the vermal lobules I–III ($x = 0$ to -6 mm,

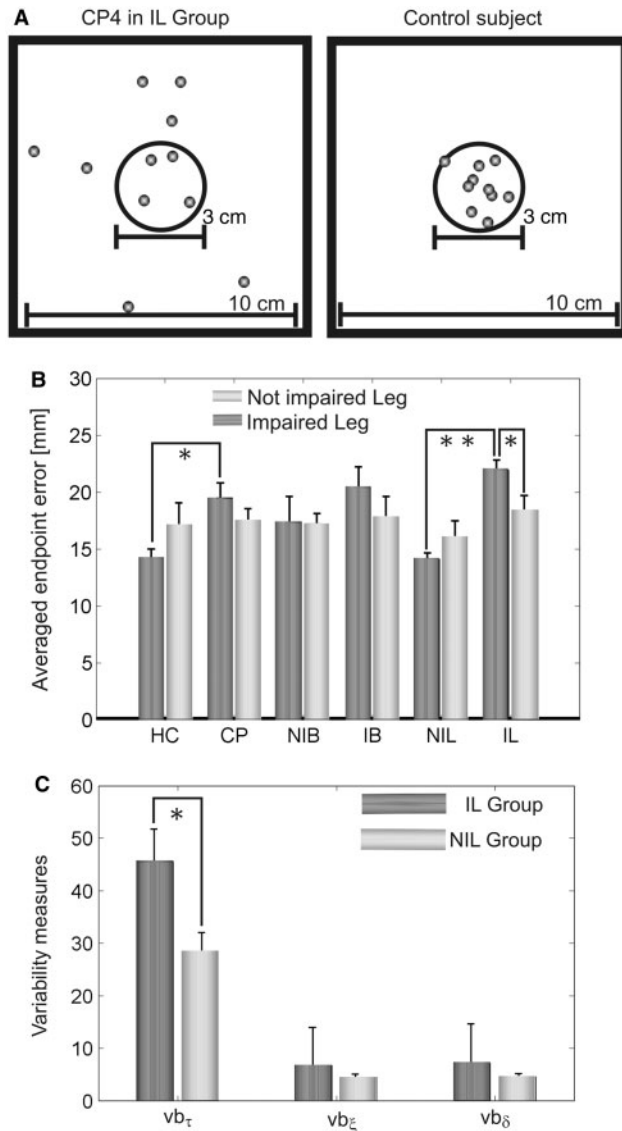


Fig. 2 (A) End-point distance error of the impaired leg for CP4 and a control subject. (B) Group comparisons of the leg placement error between HC, CP and the different patient subgroups: NIB, IB (see following section for categorization), NIL and IL. Shown is the performance for the impaired and non-impaired leg. (C) Comparison of the different variability measures vb_{τ} , vb_{ξ} and vb_{δ} for intra-limb coordination in the leg placement task. Shown are group differences for the patient subgroups with and without impaired leg placement (IL/NIL). Stars indicate significant group differences ($*P < 0.05$) and Bonferroni adjusted group difference ($**P < 0.017$).

$y = -44$ to -52 mm, $z = -22$ to -32 mm) as well as vermal lobules VIIIA, VIIIB and IX in the lower vermis ($x = -10$ to $+4$ mm, $y = -54$ to -70 mm, $z = -38$ to -48 mm).

Intra-limb coordination pattern for gait with and without additional loads

Comparing CP and HC for normal gait (Fig. 5), we found significant differences in step length ($U = 128$, $P = 0.04$).

Comparing the patient subgroups, there is, due to the categorization method, a significant difference between subgroups IB and NIB in step width ($U = 19$, $P = 0.03$) and lateral sway ($U = 19$, $P = 0.03$). In addition there is a significant difference between subgroups IL and NIL in velocity ($U = 38$, $P = 0.04$).

Attaching weights to both shanks led to comparable changes in standard gait parameters in HC and in the different patient subgroups. Figure 5 shows standard gait parameters for normal gait, for the first and third adaptation trial with weights as well as for the first and third post-adaptation trial after removing the weights. Changes in step length, velocity, lateral sway and step width were comparable for controls and the different patient subgroups. In particular, step length was decreased compared to normal gait in both adaptation and post-adaptation trials for all subject groups.

Analysing the changes in intra-limb coordination using angle-angle plots reveals first hints of differences in adaptation behaviour (Fig. 6). For the healthy control subject HC1, one can identify a specific change in the hip–knee coordination pattern of the first recorded gait cycle in the adaptation trial, in particular in the phase of mid and terminal swing (label 1). In the following steps, the coordination patterns converge to those of normal walking. The first gait cycle of the post-adaptation trials reveals differences of the coordination pattern in the gait phases of terminal stance and pre-swing (label 2). Also for the post-adaptation trials, the coordination patterns converge to those of normal walking. Note that both reported changes in coordination patterns and their adaptation within subsequent trials can also be observed (to a smaller degree) in Patient CP6, a characteristic patient of the NIL subgroup.

In contrast to this, CP10, a characteristic patient of the IL subgroup, shows a clear change in hip–knee coordination pattern for adaptation and post-adaptation trials in the gait phases of mid and terminal swing (label 3). Contrasting with the control subject HC1 and patient CP6, the pattern did not change in subsequent trials.

In order to analyse the differences in intra-limb coordination quantitatively, we computed in particular changes in temporal characteristics for adaptation trials (vb_{τ}^{adapt} , vb_{ξ}^{adapt}) and post-adaptation trials (vb_{τ}^{post} , vb_{ξ}^{post}) in comparison to an averaged trajectory of normal walking as reference (see Methods section). Results for temporal variability vb_{τ}^{adapt} for the different subgroups are illustrated in Fig. 7A. There were no significant differences between the groups for temporal variability vb_{τ}^{adapt} or spatial variability vb_{ξ}^{adapt} on the first adaptation trial ($P > 0.20$). This finding implies that in the first adaptation trial there was no difference in the intra-limb coordination between HC and the various patient subgroups. For all subgroups, the temporal difference in intra-limb coordination vb_{τ}^{adapt} is significantly increased in comparison with the baseline variability in normal walking vb_{τ} .

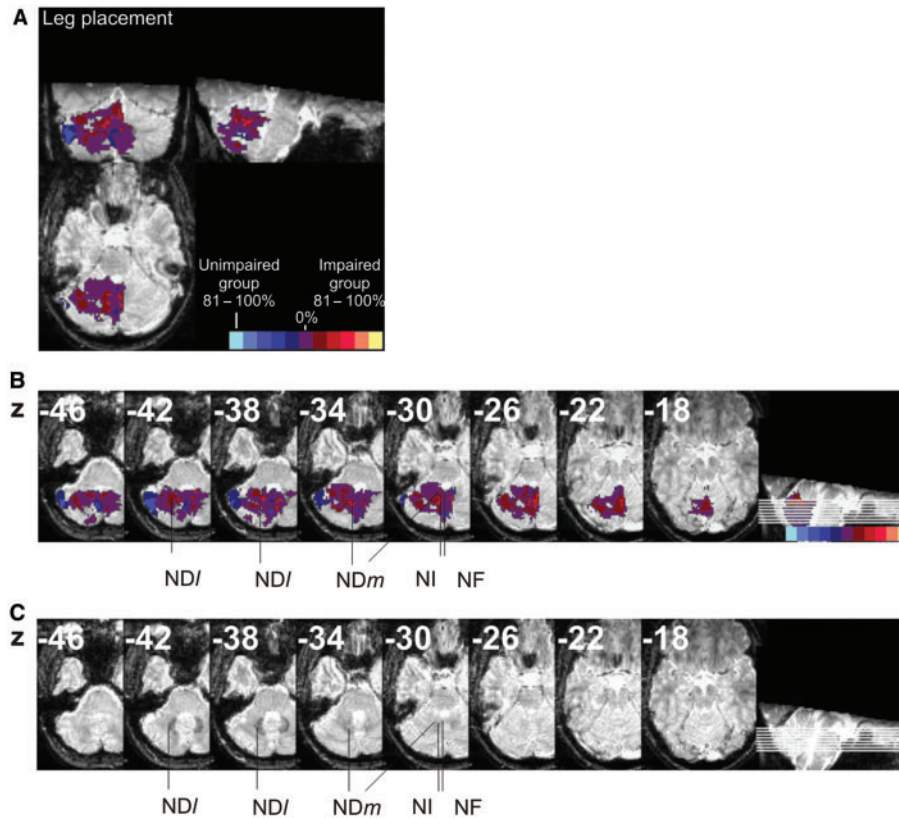


Fig. 3 Subtraction of regions of interest between the patient groups with IL and NIL. Shown are transverse, coronal and sagittal views (**A**) and additional transverse views (**B**). The percentage subtraction shows eleven levels of ROI: each bar represents 20% increments. Yellow represents 81–100% impaired group. Regions affected to the same proportion in both patient groups are marked in purple (0%) (NDI = ventrolateral dentate nucleus, NDm = dorsomedial dentate nucleus). (**C**) Cerebellar nuclei are shown as hypointensities in the utilized MRI template. This template has been taken out of the MRI atlas of the cerebellar nuclei published by our group (Dimitrova et al., 2002).

On the third trial there is evidence of adaptation in the intra-limb coordination pattern for the control group, as shown by a significantly reduced temporal difference vb_{τ}^{adapt} ($U=91$, $P=0.01$) in comparison to the first trial (Fig. 7A). Furthermore, vb_{τ}^{adapt} shows values comparable to the baseline variability of normal walking.

In order to quantify the adaptation behaviour over all three trials with weights, we defined an adaptation index

$$I_{\tau}^{\text{adapt}} = \frac{vb_{\tau}^{\text{adapt}}(\text{trial}_1) - vb_{\tau}^{\text{adapt}}(\text{trial}_3)}{vb_{\tau}^{\text{adapt}}(\text{trial}_1)} \quad (4)$$

Positive values of this index indicate that the temporal aspects of intra-limb coordination were adapted, thus resembling more those of normal walking, than in the first trial after attaching the weights. For this adaptation index, we identified significant group differences between HC and CP ($U=11$, $P=0.009$) as well as between patient subgroups with and without impaired leg placement (IL/NIL) ($U=41$, $P=0.008$), but not between patient subgroups with and without impaired balance (IB/NIB) (the fact that the adaptation index for the IB group is on average negative can be explained by the overlap of the patients groups

IB and IL). These results imply that the adaptation of intra-limb coordination is especially reduced in the IL group (Fig. 7C).

In order to test for after-effects, we also analysed three post-adaptation trials after removing the weights. The measure vb_{τ}^{post} quantifies the changes of the temporal characteristics of hip–knee coordination after removing the weights. The parameter vb_{τ}^{post} was significantly increased for the first compared to the third post-adaptation trial for controls ($U=52$, $P=0.04$) as well as for the NIL subgroup ($U=26$, $P=0.02$), but not for the IL subgroup (Fig. 7B). The comparison of vb_{τ}^{post} to the baseline variability of normal walking vb_{τ} shows, that on the first post-adaptation trial the temporal aspects of intra-limb coordination had not yet been deadapted. For the third trial, the vb_{τ}^{post} reached the variability baseline vb_{τ} for both controls and NIL subgroup.

Correspondingly to the adaptation index in Equation (4) we quantified the deadaptation behaviour computing a post-adaptation index:

$$I_{\tau}^{\text{post}} = \frac{vb_{\tau}^{\text{post}}(\text{trial}_1) - vb_{\tau}^{\text{post}}(\text{trial}_3)}{vb_{\tau}^{\text{post}}(\text{trial}_1)} \quad (5)$$

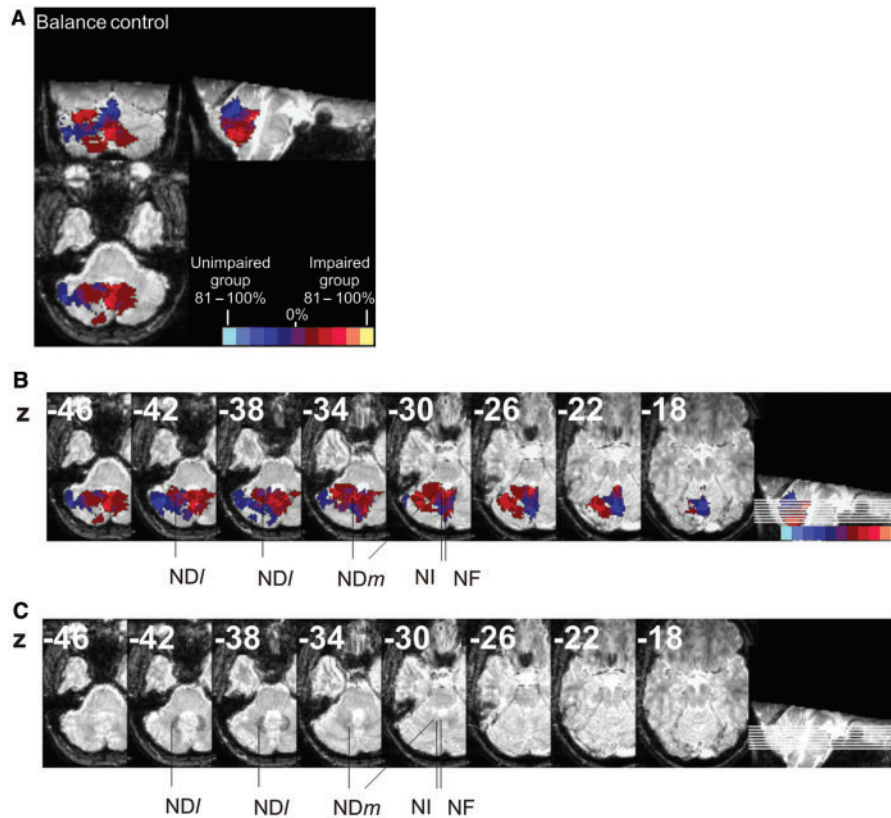


Fig. 4 Subtraction of regions of interest between patient groups with impaired balance and unimpaired balance in gait. Shown are transverse, coronal and sagittal views (A) and additional transverse views (B). (C) Cerebellar nuclei are shown as hypointensities in the utilized MRI template. This template has been taken out of the MRI atlas of the cerebellar nuclei published by our group (Dimitrova et al., 2002).

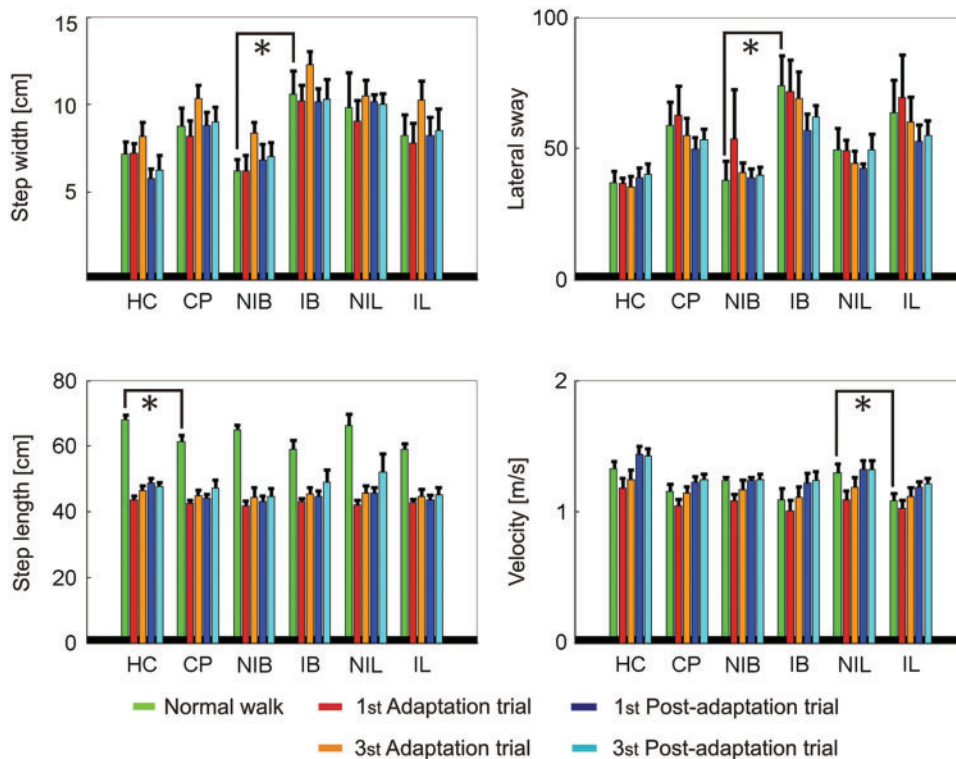


Fig. 5 Comparison of the most important standard gait parameters for normal walking, the first and the third adaptation trial (with weights) and the first and the third post-adaptation trial (without weights). Stars denote statistical significance ($P < 0.05$).

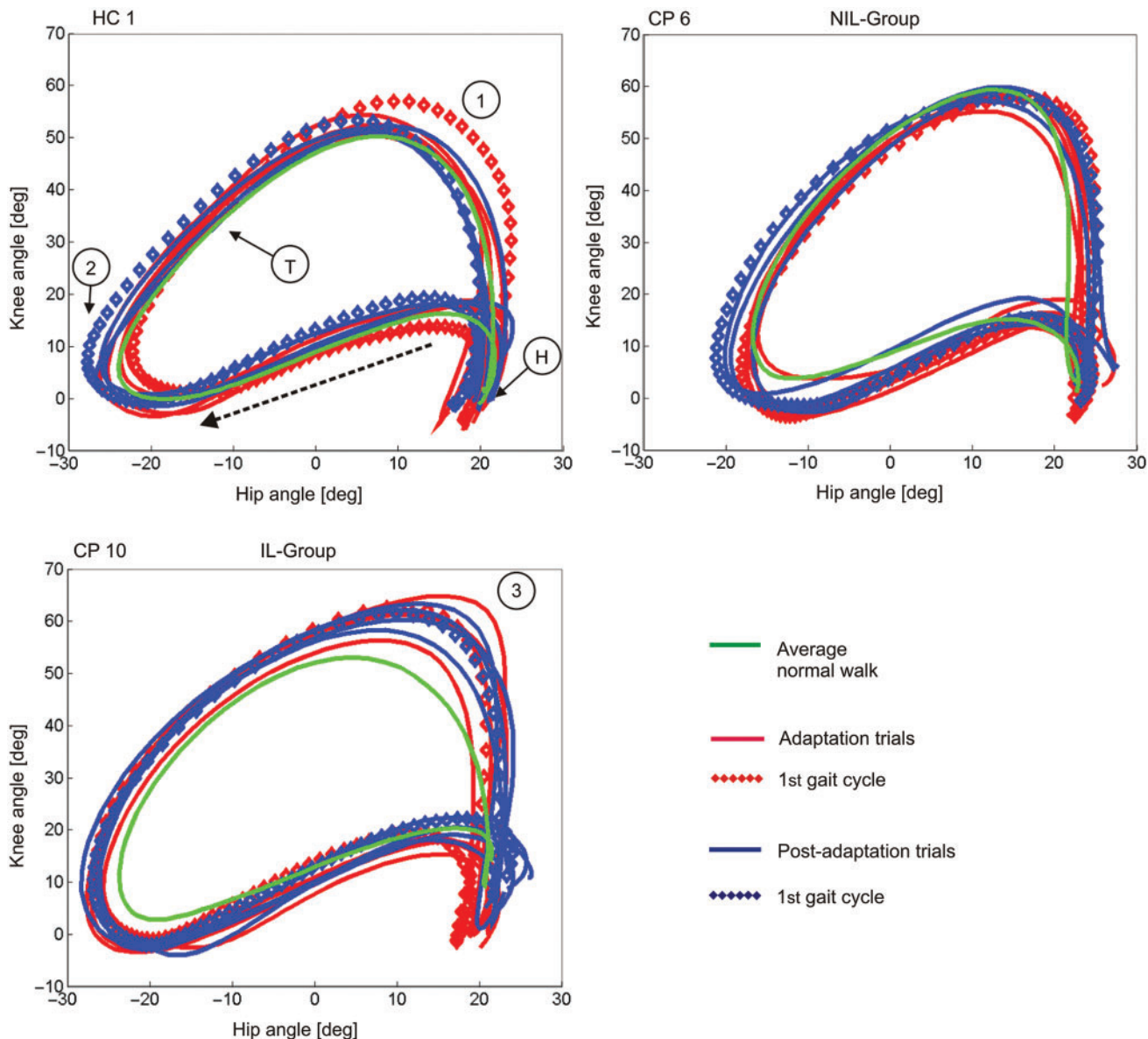


Fig. 6 Angle–angle plots for a control subject and two patients. Illustrated is the intra-limb coordination of knee and hip angles for gait cycles in normal walking, adaptation trials with weight and post-adaptation trials without weight. Plotted are an averaged trajectory for normal walking and five gait cycles for adaptation trials and post-adaptation trials. The first recorded gait cycles for both adaptation and post-adaptation trials are marked with diamonds. Label (H) indicates the heel strike at the beginning of the stance phase, and label (T) the toe-off event at the beginning of the swing phase. The dotted arrow indicates the stance phase. The control subject HC1 shows specific changes in the coordination patterns for the first gait cycles of adaptation trials (label 1) and post-adaptation trials (label 2). Patient CP6 shows similar changes of coordination patterns, but to a smaller degree. In contrast, CP10 shows strongly increased variability, especially in the gait phases of mid and terminal swing for the adaptation trials (label 3) (see Results section for further description).

For this post-adaptation index, significant group differences between controls and patients ($U=80$, $P=0.03$) were observed as well as between IL and NIL patient subgroups ($U=40$, $P=0.01$). This finding indicates an after-effect in the intra-limb coordination for HC and NIL subgroup. Adaptation of intra-limb coordination was significantly reduced in the IL group (Fig. 7C).

Since our measures in general determine the variability of intra-limb coordination over whole gait cycles, a more

detailed analysis was performed for distinguishing the abnormalities in intra-limb coordination during adaptation and post-adaptation trials. Therefore, we examined the temporal measures vb_{τ}^{adapt} and vb_{τ}^{post} for different phases of the gait cycles (see Methods section). This analysis revealed that the biggest differences of vb_{τ}^{adapt} exist during mid swing and terminal swing (73–100% of gait cycle; $t_{22}=2.8$, $P=0.01$). This result is consistent with Fig. 6 that shows changes of the coordination patterns during

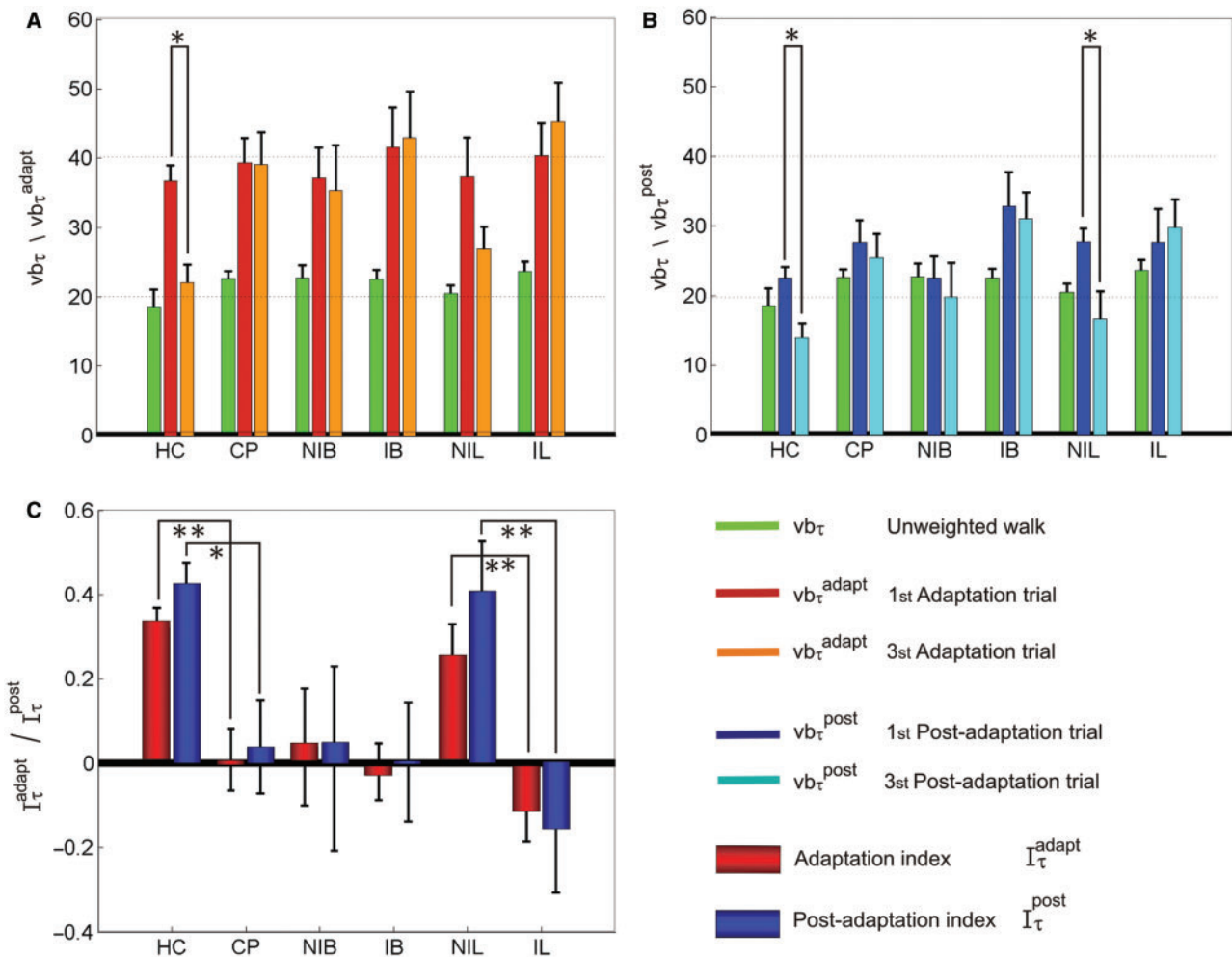


Fig. 7 (A) Temporal differences in intra-limb coordination (vb_{τ}^{adapt}) for the first and third adaptation trial in comparison to the temporal variability of normal walking (vb_{τ}) for the different patient groups. Shown are the values for the intra-limb coordination of hip and knee angle of the impaired leg. (B) Temporal differences in intra-limb coordination (vb_{τ}^{post}) for the first and third post-adaptation trial in comparison to the temporal variability of normal walking (vb_{τ}). (C) Adaptation index I_{τ}^{adapt} and post-adaptation index I_{τ}^{post} Equation (4) for the different patient subgroups. Stars indicate significant group differences ($*P < 0.05$), and Bonferroni-adjusted group difference ($**P < 0.017$) (see Results section for further description).

adaptation specifically for these gait phases. In contrast, vb_{τ}^{post} exhibits the biggest differences during pre-swing and initial swing (50–73% of gait cycle; $t_{22} = 1.84$, $P = 0.04$), also consistent with the coordination patterns shown in Fig. 6.

Relationship between impairments in gait adaptation and voluntary leg placement

A strong negative correlation ($r = -0.76$, $P = 0.004$) exists between the leg placement error and the adaptation capability (Fig. 8). This result suggests that impairments in leg placement and changes in the adaptation of the intra-limb coordination patterns have a strong pathophysiological association.

Discussion

Functional localization of dynamic balance control

We demonstrated correlations of specific balance-related parameters in gait with cerebellar lesion sites, in particular the NF. Consistently with existing results from animal (e.g. Thach *et al.*, 1992; Chambers and Sprague, 1955a, b) and human studies (Dichgans and Diener, 1984; Bastian *et al.*, 1998), our results support the hypothesis that the medial zone of the cerebellum is involved in dynamic balance control during gait. Although the most significant difference between the affected and unaffected balance groups was that lesions of the NF (and inferior vermis) were most prominent in the affected group, lesions of the NI and vermal lobules I–III were also more common.

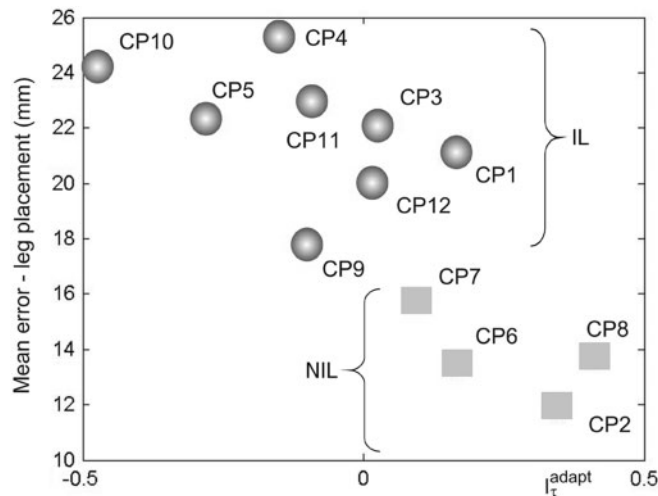


Fig. 8 The mean error in the voluntary leg placement task plotted against the adaptation index. Indicated are the two patient subgroups with IL and NIL.

Similar observations have been made in our previous studies in patients with chronic surgical lesions correlating MRI data and clinical ataxia scores (Schoch *et al.*, 2006) and postural sway using dynamic posturography in patients with chronic focal lesions (Konczak *et al.*, 2005). In both studies we found that impaired balance control was related to NF and adjacent NI lesions. These results are consistent with the hypothesis that balance control may be related to inter-joint coordination even in standing (e.g. Horak and Nashner, 1986; Kuo and Zajac, 1993; Park *et al.*, 2004; Hsu *et al.*, 2007). For example, balancing in response to backward platform displacements evokes ‘ankle’ and ‘ankle-hip’ balancing strategies (Horak and Nashner, 1986). Effective inter-joint coordination may be required for the latter.

Beyond the importance of truncal control, dynamic balance in gait is also supposed to be influenced by foot placement (e.g. Townsend, 1985; Winter, 1992, 1995; Bauby and Kuo, 2000). Presumably lateral sway during walking is strongly affected by the placement of feet on the ground. Excessively lateral foot placement causes the centre of mass to deviate toward the opposite leg on the next stride. Excessively medial placement of a leg creates a risk of falling laterally over the medially placed foot.

Our results confirm such an influence of disturbed leg placement on dynamic balance. This phenomenon would explain the data of CP3 who was categorized as belonging to both the IB and IL subgroups. Since the ND was the only affected nucleus for this patient (Table 2), one would have expected him to be impaired in leg placement rather than in dynamic balance control. An influence of leg placement deficits on dynamic balance would explain the observed large lateral sway for this patient (Table 3).

Thus, our data suggests that, beyond the well-established importance of the medial zone of the cerebellum in truncal

control, dynamic balance in gait is also influenced by the intermediate and potentially the lateral zone by contributing to inter-joint coordination for balance control and adequate foot placement.

Functional localization of goal-directed leg control

Whereas balance control during gait is suggested to depend both on truncal and on limb control, the leg placement task performance in our experimental setup depended primarily on limb control. We were able to show that patients with deficits in leg placement (that is inter-limb coordination) are more likely to have lesions of the interposed (NI) and adjacent dentate nuclei (ND). There was no indication in MRI subtraction analysis that the NF played an additional role in the leg placement task.

These findings are consistent with a previous study showing a significant correlation between the clinical degree of lower (and upper) limb ataxia and lesions of the NI and adjacent ND (Schoch *et al.*, 2006). In addition, several animal lesion studies revealed an influence of the interposed nuclei on the control of goal-directed limb movements (van Kan *et al.*, 1993; Chambers and Sprague, 1955b; Milak *et al.*, 1997; Bracha *et al.*, 1999; Cooper *et al.*, 2000; Apps and Garwicz, 2005). The influence of the ND might be explained by different factors. On the one hand, there is neuroanatomical evidence that adjacent dorsomedial regions of the ND exhibit properties similar to those of the interposed nuclei, and that they may also be part of the intermediate zone (Mason *et al.*, 1998). On the other hand, lateral regions and the ND have been shown to be important for visually guided movements (Stein and Glickstein, 1992; Armstrong *et al.*, 1997; Cerminara *et al.*, 2005).

In contrast, lesions of the vermis and NF are commonly reported to have only a minor influence on goal-directed limb movements (Dichgans and Diener, 1984; Thach *et al.*, 1992). This view is consistent with the fact that we did not find differences in leg placement performance between patients with and without balance impairments.

Abnormalities in intra-limb coordination

Our analysis of intra-limb coordination patterns revealed related abnormalities for different movements. The patients who were categorized as impaired in leg placement showed abnormalities in the temporal characteristics of joint coordination patterns for the leg placement as well as for the adaptive walking task. The significant correlation ($r = -0.76$, $P = 0.004$) between leg placement performance and adaptation index indicates a strong functional relationship between both movement tasks.

In the current study, the temporal variability measure vb_{τ} was not significantly increased in patients with cerebellar lesions compared with HC for gait without

weights ($P > 0.17$). This finding is in contrast with a previous study where we found significantly increased values of this parameter for patients with more severe ataxia (mean ICARS 28.1 compared with 5.7 in this study) (Ilg et al., 2007). The difference in the outcome of the two studies is consistent with the view that deficits related to leg control become more obvious in more difficult walking tasks (Morton and Bastian, 2003) or for more severe forms of ataxia.

The observed abnormalities in the adaptation of intra-limb coordination to the weights are consistent with previous studies on the adaptation of locomotor patterns, showing a decreased adaptation for cerebellar patients (Rand et al., 1998; Earhart and Bastian, 2001; Morton and Bastian, 2006).

In our adaptive walking task, on the one hand, patients and controls showed comparable changes of general gait parameters such as step length and velocity. Since these gait parameters showed immediate rather than gradual changes, they might be influenced mainly by higher-order compensation strategies such as decreasing step length, or load-related feedback control loops (Fig. 5). On the other hand, temporal characteristics of intra-limb coordination changed gradually across trials, converging towards the normal coordination pattern in both controls and the NIL patient subgroup, but significantly less in the IL subgroup. For the controls and NIL subgroup, the significant increase of the measure vb_{τ}^{post} for the first post-adaptation trial indicates an after-effect on the temporal characteristics of intra-limb coordination. These results are consistent with the hypothesis that the recalibration of feedforward control mechanisms (see Bastian, 2006 for review) might play a role for the observed adaptation processes.

The lack of adaptive modification of locomotion for the IL patients could also be partly influenced by compensation strategies such as stiffening of the knee joint in order to reduce the impairments in intra-limb coordination. However, since all patients showed comparable data for the parameters step length and peak angles, such strategies do not seem to be the main reason for the observed changes in the adaptation of intra-limb coordination patterns. Furthermore, the cerebellum has been proposed to be involved in sensory perception and disordered proprioceptive perception may influence the adaptation of locomotor patterns. A more recent study (Maschke et al., 2003), however, found unimpaired kinaesthesia in patients with cerebellar degeneration. Although no specific laboratory testing has been performed, standard clinical examinations revealed no abnormalities of vibration sense and joint-position sense in our patients (see Methods section).

In summary, our data indicate that those ataxic patients who are impaired in goal-directed leg placement also exhibit changes in the adaptation of intra-limb coordination in locomotion. We hypothesize that these defects may be influenced by impairments in the control mechanisms relevant for both goal-directed movements and adaptive locomotion, depending at least partly on the integrity of the intermediate zone of the cerebellum. Such an involvement

of the intermediate zone view is consistent with animal locomotion studies (e.g. Udo et al., 1980; Yu and Eidelberg, 1983; Bracha et al., 1999) and neuroanatomical evidence in cats [the intermediate region is known to receive direct information from somatosensory receptors and spinal motor programmes through spinocerebellar tracts and spinoreticulocerebellar pathways and projects back to spinal cord pattern generators (Bloedel and Courville, 1981; Brooks and Thach, 1981; Arshavsky et al., 1983; Bosco and Poppele, 2001)].

In conclusion, our findings provide the first demonstration of the influence of the intermediate zone on intra-limb coordination in human locomotion and goal-directed leg placement. Furthermore, it seems likely that, beyond the well-known and confirmed role of the medial zone, the intermediate (and potentially the lateral) zone are involved in dynamic balance control in locomotion.

More generally, our study support the hypothesis that since bipedal locomotion is less stable than quadrupedal locomotion it might require additional supraspinal control mechanisms in order to stabilize dynamic balance (Orlovsky et al., 1999; Morton and Bastian, 2003). The intermediate and the lateral zone of the cerebellum might play a significant role in these supraspinal control circuits.

Supplementary material

Supplementary material is available at *Brain* online.

Acknowledgements

We thank T. Wiestler, A. Hogan, B. Brol and C. Roether for help with data acquisition and data analysis. Special thanks to L. Schöls for insightful comments.

Funding

Deutsche Forschungsgemeinschaft (DFG TI 239/5-2); Volkswagenstiftung; Hermann and Lilly Schilling Foundation; Werner-Reichardt Centre for Integrative Neuroscience and EC FP6 project COBOL (to W.I. and M.G.).

References

- Apps R, Garwicz M. Anatomical and physiological foundations of cerebellar information processing. *Nat Rev Neurosci* 2005; 6: 297–311.
- Armstrong DM, Apps R, Marple-Horvat DE. Aspects of cerebellar function in relation to locomotor movements. *Prog Brain Res* 1997; 114: 401–21.
- Arshavsky YI, Gelfand IM, Orlovsky GN. The cerebellum and control of rhythmical movements. *Trends Neurosci* 1983; 6: 417–22.
- Bastian AJ. Learning to predict the future: the cerebellum adapts feedforward movement control. *Curr Opin Neurobiol* 2006; 16: 645–49.
- Bastian AJ, Martin TA, Keating JG, Thach WT. Cerebellar ataxia: abnormal control of interaction torques across multiple joints. *J Neurophysiol* 1996; 76: 492–509.
- Bastian AJ, Mink JW, Kaufman BA, Thach WT. Posterior vermal split syndrome. *Ann Neurol* 1998; 44: 601–10.
- Bauby CE, Kuo AD. Active control of lateral balance in human walking. *J Biomech* 2000; 33: 1433–40.
- Bloedel JR, Courville J. Cerebellar afferent systems. In: Brooks VB, editor. *Handbook of physiology, the nervous system*. Bethesda: American Physiological Society; 1981. p. 735–830.

- Bosco G, Poppele RE. Proprioception from a spinocerebellar perspective. *Physiol Rev* 2001; 81: 539–68.
- Bracha V, Kolb FP, Irwin KB, Bloedel JR. Inactivation of interposed nuclei in the cat: classically conditioned withdrawal reflexes, voluntary limb movements and the action primitive hypothesis. *Exp Brain Res* 1999; 126: 77–92.
- Brett M, Leff AP, Rorden C, Ashburner J. Spatial normalization of brain images with focal lesions using cost function masking. *Neuroimage* 2001; 14: 486–500.
- Brooks V, Thach WT. Cerebellar control of posture and movement. In: Brooks V, editor. *Handbook of physiology: motor control*. Washington DC: American Physiology Society; 1981. p. 877–946.
- Cerminara NL, Edge AL, Marple-Horvat DE, Apps R. The lateral cerebellum and visuomotor control. *Prog Brain Res* 2005; 148: 213–26.
- Chambers WW, Sprague JM. Functional localization in the cerebellum. I. Organization in longitudinal cortico-nuclear zones and their contribution to the control of posture, both extrapyramidal and pyramidal. *J Comp Neurol* 1955a; 103: 105–29.
- Chambers WW, Sprague JM. Functional localization in the cerebellum. II. Somatotopic organization in cortex and nuclei. *AMA Arch Neurol Psychiatry* 1955b; 74: 653–80.
- Cooper SE, Martin JH, Ghez C. Effects of inactivation of the anterior interpositus nucleus on the kinematic and dynamic control of multijoint movement. *J Neurophysiol* 2000; 84: 1988–2000.
- Dichgans J, Diener HC. Clinical evidence for functional compartmentalization of the cerebellum. In: Bloedel JR, Dichgans J, Precht W, editors. *Cerebellar functions*. Berlin: Springer; 1984. p. 126–47.
- Diedrichsen J, Hashambhoy Y, Rane T, Shadmehr R. Neural correlates of reach errors. *J Neurosci* 2005; 25: 9919–31.
- Dimitrova A, Weber J, Redies C, Kindsvater K, Maschke M, Kolb FP, et al. MRI atlas of the human cerebellar nuclei. *Neuroimage* 2002; 17: 240–55.
- Dum RP, Strick PL. An unfolded map of the cerebellar dentate nucleus and its projections to the cerebral cortex. *J Neurophysiol* 2003; 89: 634–9.
- Earhart GM, Bastian AJ. Selection and coordination of human locomotor forms following cerebellar damage. *J Neurophysiol* 2001; 85: 759–69.
- Giese MA, Poggio T. Morphable models for the analysis and synthesis of complex motion patterns. *Int J Comp Vis* 2000; 38: 59–73.
- Hallett M, Massaquoi SG. Physiologic studies of dysmetria in patients with cerebellar deficits. *Can J Neurol Sci* 1993; 20 (Suppl 3): S83–92.
- Horak FB, Nashner LM. Central programming of postural movements: adaptation to altered support-surface configurations. *J Neurophysiol* 1986; 55: 1369–81.
- Hsu WL, Scholz JP, Schoner G, Jeka JJ, Kiemel T. Control and estimation of posture during quiet stance depends on multijoint coordination. *J Neurophysiol* 2007; 97: 3024–35.
- Ilg W, Golla H, Thier P, Giese MA. Specific influences of cerebellar dysfunctions on gait. *Brain* 2007; 130: 786–98.
- Karnath HO, Himmelbach M, Rorden C. The subcortical anatomy of human spatial neglect: putamen, caudate nucleus and pulvinar. *Brain* 2002; 125: 350–60.
- Kirtley C. *Clinical gait analysis - theory and practice*. London, UK: Elsevier Churchill Livingstone; 2006.
- Konczak J, Schoch B, Dimitrova A, Gizewski E, Timmann D. Functional recovery of children and adolescents after cerebellar tumour resection. *Brain* 2005; 128: 1428–41.
- Kuo AD, Zajac FE. Human standing posture: multi-joint movement strategies based on biomechanical constraints. *Prog Brain Res* 1993; 97: 349–58.
- Maschke M, Gomez CM, Ebner TJ, Konczak J. Hereditary cerebellar ataxia progressively impairs force adaptation during goal-directed arm movements. *J Neurophysiol* 2004; 91: 230–8.
- Maschke M, Gomez CM, Tuite PJ, Konczak J. Dysfunction of the basal ganglia, but not the cerebellum, impairs kinaesthesia. *Brain* 2003; 126: 2312–22.
- Mason CR, Miller LE, Baker JF, Houk JC. Organization of reaching and grasping movements in the primate cerebellar nuclei as revealed by focal muscimol inactivations. *J Neurophysiol* 1998; 79: 537–54.
- Milak MS, Shimansky Y, Bracha V, Bloedel JR. Effects of inactivating individual cerebellar nuclei on the performance and retention of an operantly conditioned forelimb movement. *J Neurophysiol* 1997; 78: 939–59.
- Morton SM, Bastian AJ. Cerebellar contributions to locomotor adaptations during splitbelt treadmill walking. *J Neurosci* 2006; 26: 9107–16.
- Morton SM, Bastian AJ. Relative contributions of balance and voluntary leg-coordination deficits to cerebellar gait ataxia. *J Neurophysiol* 2003; 89: 1844–56.
- Morton SM, Dordevic GS, Bastian AJ. Cerebellar damage produces context-dependent deficits in control of leg dynamics during obstacle avoidance. *Exp Brain Res* 2004; 156: 149–63.
- Noble JW, Prentice SD. Adaptation to unilateral change in lower limb mechanical properties during human walking. *Exp Brain Res* 2005; 1–14.
- Orlovsky GN, Deliagina TG, Grillner S. *Neural control of locomotion: from mollusc to man*. Oxford, UK: Oxford University Press; 1999.
- Palliyath S, Hallett M, Thomas SL, Lebediewska MK. Gait in patients with cerebellar ataxia. *Mov Disord* 1998; 13: 958–64.
- Park S, Horak FB, Kuo AD. Postural feedback responses scale with biomechanical constraints in human standing. *Exp Brain Res* 2004; 154: 417–27.
- Rand MK, Wunderlich DA, Martin PE, Stelmach GE, Bloedel JR. Adaptive changes in responses to repeated locomotor perturbations in cerebellar patients. *Exp Brain Res* 1998; 122: 31–43.
- Rorden C, Karnath HO, Bonilha L. Improving lesion-symptom mapping. *J Cogn Neurosci* 2007; 19: 1081–88.
- Schmahmann JD, Dojon J, Toga AW, Petrides M, Evans AC. *MRI Atlas of the human cerebellum*. San Diego: Academic Press; 2000.
- Schoch B, Dimitrova A, Gizewski ER, Timmann D. Functional localization in the human cerebellum based on voxelwise statistical analysis: a study of 90 patients. *Neuroimage* 2006; 30: 36–51.
- Schoch B, Gorissen B, Richter S, Ozimek A, Kaiser O, Dimitrova A, et al. Do children with focal cerebellar lesions show deficits in shifting attention? *J Neurophysiol* 2004; 92: 1856–66.
- Smith MA, Shadmehr R. Intact ability to learn internal models of arm dynamics in Huntington's disease but not cerebellar degeneration. *J Neurophysiol* 2005; 93: 2809–21.
- Stein JF, Glickstein M. Role of the cerebellum in visual guidance of movement. *Physiol Rev* 1992; 72: 967–1017.
- Stergiou N, editor. *Innovative analyses of human movement*. Human Kinetics; 2004.
- Stolze H, Klebe S, Petersen G, Raethjen J, Wenzelburger R, Witt K, et al. Typical features of cerebellar ataxic gait. *J Neurol Neurosurg Psychiatry* 2002; 73: 310–2.
- Sullivan EV, Rose J, Pfefferbaum A. Effect of vision, touch and stance on cerebellar vermian-related sway and tremor: a quantitative physiological and MRI study. *Cereb Cortex* 2006; 16: 1077–86.
- Thach WT, Bastian AJ. Role of the cerebellum in the control and adaptation of gait in health and disease. *Prog Brain Res* 2004; 143: 353–66.
- Thach WT, Goodkin HP, Keating JG. The cerebellum and the adaptive coordination of movement. *Annu Rev Neurosci* 1992; 15: 403–42.
- Topka H, Konczak J, Schneider K, Boose A, Dichgans J. Multijoint arm movements in cerebellar ataxia: abnormal control of movement dynamics. *Exp Brain Res* 1998; 119: 493–503.
- Townsend MA. Biped gait stabilization via foot placement. *J Biomech* 1985; 18: 21–38.
- Trouillas P, Takayanagi T, Hallett M, Currier RD, Subramony SH, Wessel K, et al. International Cooperative Ataxia Rating Scale for pharmacological assessment of the cerebellar syndrome. The Ataxia Neuropharmacology Committee of the World Federation of Neurology. *J Neurol Sci* 1997; 145: 205–11.
- Udo M, Matsukawa K, Kamei H, Oda Y. Cerebellar control of locomotion: effects of cooling cerebellar intermediate cortex in high decerebrate and awake walking cats. *J Neurophysiol* 1980; 44: 119–34.
- van Kan PL, Houk JC, Gibson AR. Output organization of intermediate cerebellum of the monkey. *J Neurophysiol* 1993; 69: 57–73.
- Winter DA. Foot trajectory in human gait: a precise and multifactorial motor control task. *Phys Ther* 1992; 72: 45–53; discussion 54–6.
- Winter DA. Human balance and posture control during standing and walking. *Gait Posture* 1995; 3: 193–214.
- Yu J, Eidelberg E. Recovery of locomotor function in cats after localized cerebellar lesions. *Brain Res* 1983; 273: 121–31.